

Article

New Copper(II)-L-Dipeptide-Bathophenanthroline Complexes as Potential Anticancer Agents—Synthesis, Characterization and Cytotoxicity Studies—And Comparative DNA-Binding Study of Related Phen Complexes

Carlos Y. Fernández^{1,2}, Natalia Alvarez¹ , Analu Rocha³, Javier Ellena⁴ , Antonio J. Costa-Filho⁵, Alzir A. Batista³ and Gianella Facchin^{1,*} 

¹ Facultad de Química, Universidad de la República, Av. General Flores 2124, CC1157, Montevideo 11800, Uruguay

² Programa de Posgrados de la Facultad de Química, Universidad de la República, Av. General Flores 2124, Montevideo 11800, Uruguay

³ Departamento de Química, Universidade Federal de São Carlos, CP 676, São Carlos 13565-905, SP, Brazil

⁴ Instituto de Física de São Carlos, Universidade de São Paulo, Av. do Trabalhador São-Carlense 400, São Carlos 143566-590, SP, Brazil

⁵ Faculdade de Filosofia, Ciências e Letras de Ribeirão Preto, Universidade de São Paulo, Av. Bandeirantes, Ribeirão Preto 14040-901, SP, Brazil

* Correspondence: gfacchin@fq.edu.uy



Citation: Fernández, C.Y.; Alvarez, N.; Rocha, A.; Ellena, J.; Costa-Filho, A.J.; Batista, A.A.; Facchin, G. New Copper(II)-L-Dipeptide-Bathophenanthroline Complexes as Potential Anticancer Agents—Synthesis, Characterization and Cytotoxicity Studies—And Comparative DNA-Binding Study of Related Phen Complexes. *Molecules* **2023**, *28*, 896. <https://doi.org/10.3390/molecules28020896>

Academic Editors: Carlo Santini and Maura Pellei

Received: 22 December 2022

Revised: 7 January 2023

Accepted: 11 January 2023

Published: 16 January 2023



Copyright: © 2023 by the authors. Licensee MDPI, Basel, Switzerland. This article is an open access article distributed under the terms and conditions of the Creative Commons Attribution (CC BY) license (<https://creativecommons.org/licenses/by/4.0/>).

Abstract: Searching for new copper compounds which may be useful as antitumor drugs, a series of new [Cu(L-dipeptide)(batho)] (batho:4,7-diphenyl-1,10-phenanthroline, L-dipeptide: Gly-Val, Gly-Phe, Ala-Gly, Ala-Ala, Ala-Phe, Phe-Ala, Phe-Val and Phe-Phe) complexes were synthesized and characterized. To interpret the experimental IR spectra, [Cu(ala-gly)(batho)] was modelled in the gas phase using DFT at the B3LYP/LANL2DZ level of theory and the calculated vibrational frequencies were analyzed. Solid-state characterization is in agreement with pentacoordinate complexes of the general formula [Cu(L-dipeptide)(batho)]·x solvent, similar to other [Cu(L-dipeptide)(diimine)] complexes. In solution, the major species are heteroleptic, as in the solid state. The mode of binding to the DNA was evaluated by different techniques, to understand the role of the diimine and the dipeptide. To this end, studies were also performed with complexes [CuCl₂(diimine)], [Cu(L-dipeptide)(diimine)] and free diimines, with phenanthroline, neocuproine and 3,4,7,8-tetramethylphenanthroline. The cytotoxicity of the complexes was determined on human cancer cell lines MDA-MB-231, MCF-7 (breast, the first triple negative), and A549 (lung epithelial) and non-tumor cell lines MRC-5 (lung) and MCF-10A (breast). [Cu(L-dipeptide)(batho)] complexes are highly cytotoxic as compared to cisplatin and [Cu(L-dipeptide)(phenanthroline)] complexes, being potential candidates to study their in vivo activity in the treatments of aggressive tumors for which there is no curative pharmacological treatment.

Keywords: copper complexes; dipeptide; 4,7-diphenyl-1,10-phenanthroline; DNA interaction; cytotoxic activity

1. Introduction

Cancer causes a sanitary burden, with approximately 19 million new cancer cases and almost 10 million cancer deaths a year worldwide (estimated data for 2020). Female breast cancer is the most diagnosed cancer. This global cancer burden is expected to rise to more than 28 million cases per year by 2040 [1]. Several anticancer drugs are available, but they fail to achieve the desired therapeutic effect in all patients, and cause severe side effects. Therefore, it is necessary to identify and develop more effective and safe anticancer drugs [2,3].

The development of therapeutic agents may benefit from using metal coordination compounds, to exploit their chemical and structural versatility in synergy with organic ligands. Despite that, the research on coordination compounds as drugs has remained mainly in the academic media, perhaps due to the high variety of reactivity they present, including chemical speciation [4].

The discovery of the antitumor activity of cisplatin, which presents high chances of cure of testicular cancer and aids in the treatment of other classes of cancer, led to the development of other platinum complexes for cancer treatment, and several of them are currently in clinical use. This also incentivized the research on complexes of other metals [5].

The research of copper complexes as antitumor agents started under the hypothesis that, as copper is an essential metal and there are specific metabolic routes for it, its complexes may present fewer side effects than other metals [3]. To date, research on copper complexes is performed taking into account the different mechanism of action and spectrum of activity observed when compared to available drugs [6].

This potential of copper complexes to produce antitumor compounds has led to the development of several copper complexes that present antitumor activity, even when the ligands are biologically inactive [3]. The compounds in the family Casiopeinas[®] are among the most studied copper complexes, with Casiopeina III-ia, [(Cu(II))(4,4'-dimethyl-2,2'-bipyridine)(acetylacetonate)(NO₃)(H₂O)], being tested in a clinical phase I trial in Mexico [7,8]. Another relevant compound is HydroCuP[®], [Cu(tris-hydroxymethylphosphino)₄][PF₆], which is highly selective towards cancer cells and has presented promising results in advanced preclinical studies [9–11]. Cancer stem cells (CSC) are a subset of tumor cells that can survive traditional cancer treatments and generate a progeny of differentiated cells, leading to cancer relapse. Copper complexes containing bathophenanthroline (batho) are emerging as tools to fight CSCs [12]. It has been demonstrated that a batho complex induces breast CSC immunogenic cell death [13].

The mechanism of action of copper complexes is not completely understood and includes different molecular events. The lack of specificity against a single molecular target strengthens the copper complex's ability to fight a diverse cell population such as those found in a tumor. It is accepted that most complexes produce ROS, to which tumor cells are especially susceptible. Many complexes bind to the DNA, as determined *in vitro*, which possibly, combined with ROS production, is among the first molecular events triggered by the complexes [4,14–16]. Other mechanisms are also emerging [4,14,15], among the most recent being the so-called Cuproptosis described by Tsvetkov et al. [17].

Our research group has been working to develop new copper compounds with a cytotoxic activity which may lead to anticancer agents. Different series of [Cu(L-dipeptide)(diimine)] compounds were synthesized and characterized (where diimine: phenanthroline, phen, 5-NO₂-phenanthroline, 5-NO₂-phen, neocuproine, neo and 3,4,7,8-tetramethylphenanthroline, tmp) [18–22]. In general, they are potent cytotoxic agents, more active than cisplatin, with neo and tmp complexes being the most active of the group. We look forward to developing compounds with improved spectra of activity against cancer cells. In this work, we selected batho as a diiminic ligand due to references to batho complexes with high activity against cancer cells, including CSCs [12], trying to merge its activity with that of the Cu-dipeptide complexes, which are also a very stable scaffold to bind the diimine [23]. The set of L-dipeptides (L-dipeptides: Gly-Gly, Gly-Phe, Ala-Gly, Ala-Ala, Ala-Phe, Val-Phe, Phe-Ala and Phe-Phe) was selected to cover a range of different side chains and lipophilicity. The complexes were characterized both in the solid state and in aqueous solution. The complex [Cu(ala-gly)(batho)] was modelled in the gas phase using DFT, and the calculated vibrational frequencies were analyzed in order to interpret the experimental IR spectra. The binding of the complexes to the DNA was studied by UV, determining *K_b*, and viscosity methods. To evaluate the effect of the phen substituents in the DNA-binding characteristics, related complexes of phen, neo, and tmp were also included in this study. Finally, the cytotoxicity of the complexes was evaluated against

MDA-MB-231, MCF-7 (human metastatic breast adenocarcinomas, the first triple negative), MCF-10A (human non-tumor breast cells), A549 (human lung epithelial carcinoma) and MRC-5 (human non-tumor lung epithelial cells).

2. Results and Discussion

As described in the experimental section, eight new complexes—[Cu(L-Gly-Val)(batho)]·CH₃CH₂OH·3H₂O, **1**; [Cu(L-Gly-Phe)(batho)]·CH₃CH₂OH·5.5H₂O, **2**; [Cu(L-Ala-Gly)(batho)]·3H₂O, **3**; [Cu(L-Ala-Ala)(batho)]·CH₃CH₂OH·4H₂O, **4**; [Cu(L-Ala-Phe)(batho)]·CH₃CH₂OH·4.5H₂O, **5**; [Cu(L-Phe-Ala)(batho)]·1.5CH₃CH₂OH·3H₂O, **6**; [Cu(L-Phe-Val)(batho)]·0.5CH₃CH₂OH·10H₂O, **7**; and [Cu(L-Phe-Phe)(batho)]·3CH₃CH₂OH·9H₂O, **8**—were obtained according to the scheme in Figure 1. When necessary, comparative studies were performed with other complexes.

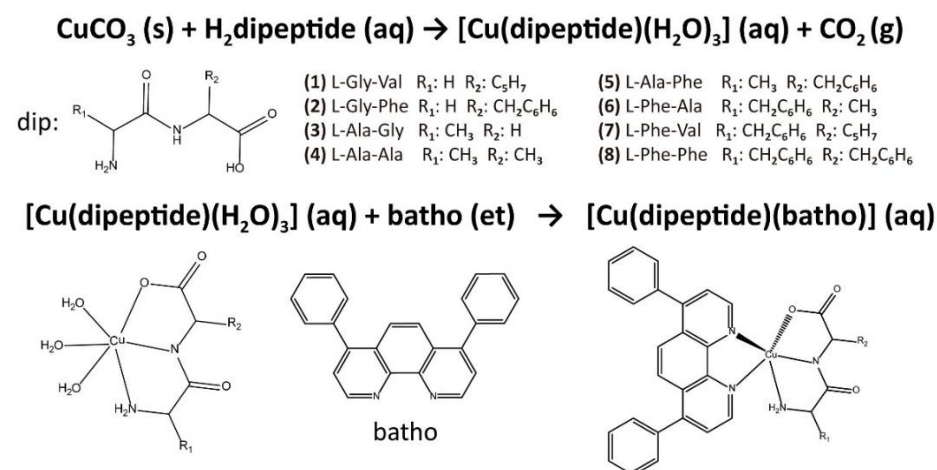


Figure 1. Scheme of the proposed structure of complexes and synthetic scheme.

2.1. Geometry Optimization, IR Spectrum Calculation, and Interpretation

To better understand the structure of the complexes and taking into account the determined structure of related complexes, the optimized geometry for [Cu(L-Ala-Gly)(batho)], corresponding to compound **3**, was calculated, confirming it referred to an energy minimum. It presents a pentacoordinate copper(II) center with a N3O equatorial coordination, where 2 N and 1 O atoms come from the dipeptide ligand, whereas the third N atom comes from the batho ligand, which is perpendicular to the plane defined by the dipeptide. The coordination and spatial arrangement are similar to those in the crystal structures of previously reported [Cu(dipeptide)(diimine)] complexes where diimine is: phen [18], 5-NO₂-phen [19], neo [20] and tmp [22]. Figure 2 presents the optimized geometry. (Figure S1, Supplementary Materials, presents a space fill representation of it.).

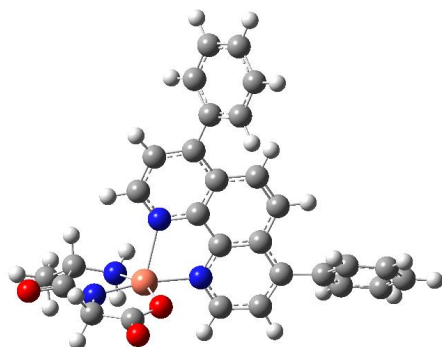


Figure 2. Optimized geometry for compound **3**.

The vibrational spectrum for compound **3** was calculated, and vibrational modes were assigned based on potential energy distribution (PED) information. The assignment and

corresponding frequencies of selected vibrational modes are shown in Table 1. For clarity purposes, the vibrational modes for bonds are discriminated by ligand (batho and dipeptide).

Table 1. Experimental band assignment using PED for **3**. Experimental and calculated frequencies are expressed in cm^{-1} .

Experimental	Calculated	PED%	Assignment	
3412	3583	99	$\nu_{\text{as}}(\text{N-H})$	
	3477	99	$\nu_{\text{s}}(\text{N-H})$	
	3252	98		
3240	3244	94		
	3238	80	$\nu_{\text{s}}, \text{ batho}(\text{C-H})$	
	3236	82		
	3235	82		
	3231	94		
	3221	81	$\nu_{\text{as}}, \text{ batho}(\text{C-H})$	
	3220	61		
	3220	85		
	3141	3212	79	
		3211	93	
3210		82		
3200		85	$\nu_{\text{as}}, \text{ batho}(\text{C-H})$	
3199		83		
3195		84		
3194		88		
3163		84		
2917	3117	93	$\nu_{\text{as}}, \text{ dipeptide}(\text{C-H})$	
	3083	99		
	3068	94	$\nu_{\text{as}}, \text{ dipeptide}(\text{C-H})$	
	3038	99	$\nu_{\text{s}}, \text{ dipeptide}(\text{C-H})$	
	3033	84		
1597	1683	77	$\delta(\text{H-N-H}) \text{ dipeptide}$	
	1662	44		
	1653	52	$\nu(\text{C-C}) \text{ batho}$	
	1652	53		
1564	1642	80	$\nu_{\text{as}}(\text{COO}) \text{ dipeptide}$	
	1621	81	$\nu(\text{N-C}) + \nu(\text{O-C}) \text{ dipeptide}$	
	1593	32	$\nu(\text{N-C}) \text{ batho}$	
1521	1526	49	$\delta(\text{H-C-C}) \text{ batho} + \text{ dipeptide}$	
	1526	64	$\delta(\text{H-C-H}) \text{ dipeptide}$	
	1521	51	$\delta(\text{H-C-C}) \text{ batho}$	
1492	1508	72		
	1499	68	$\delta(\text{H-C-H}) \text{ dipeptide}$	
	1499	29	$\tau(\text{H-C-C-O}) \text{ dipeptide}$	
	1475	49		
	1472	39	$\delta(\text{H-C-C}) \text{ batho}$	
1427	1433	87	$\delta(\text{H-C-H}) \text{ methyl in dipeptide}$	
	1404	46	$\nu(\text{N-C}) + \nu(\text{O-C}) + \nu(\text{C-C}) \text{ dipeptide}$	
	1382	40	$\tau(\text{H-C-C-N}) \text{ dipeptide}$	
1374	1379	46	$\delta(\text{H-C-C}) \text{ batho}$	
	1378	29	$\nu(\text{C-C}) \text{ batho}$	
	1378	42	$\delta(\text{H-C-C}) \text{ batho}$	
	1352	25	$\nu(\text{C-C}) \text{ batho}$	

Table 1. Cont.

Experimental	Calculated	PED%	Assignment	
1288	1335	25	δ (H-C-H) dipeptide	
	1335	50	τ (H-C-C-O) dipeptide	
	1323	55	δ (H-C-C) dipeptide	
1232	1248	58	ν_s (COO) + ν (C-C) dipeptide	
	1228	67	δ (H-C-C) batho	
	1227	65		
1183	1215	27	δ (H-C-C) batho	
	1212	49	δ (H-C-C) dipeptide	
	1212	31	τ (H-C-C-O) dipeptide	
	1209	78	δ (H-C-C) batho	
	1209	78	δ (H-C-C) batho	
1157	1130	55	ν (N-C) + ν (C-C) dipeptide	
1090	1073	49	ν (N-C) + ν (C-C) dipeptide	
1022	1047	28	τ_{oop} (H-C-C-C) batho	
	1045	62		
	1042	47		
	1025	76	δ (H-N-C) batho	
	1024	27		
	1024	34		τ_{oop} (H-C-C-N) batho
	1023	73		τ_{oop} (H-C-C-C) batho
999	1012	43	τ_{oop} (H-C-C-C) batho	
	1010	26	δ (H-C-C) dipeptide	
	1006	73	τ_{oop} (H-C-C-C) batho	
	997	53	τ (H-N-C-C) dipeptide + batho	
972	970	75	τ_{oop} (H-C-C-C) batho	
	969	69		
	910	40	δ (C-C-C) + δ (C-C-N) batho	
858	903	68	τ_{oop} (H-C-C-C) batho	
	897	84		
	895	50	τ_{oop} (H-C-C-N) batho	
	893	25		
	891	65		
	890	64		ν (N-C) + ν (C-C) + ν (O-C) dipeptide
882	66	τ_{oop} (H-C-C-C) batho		
843	851	45	ν (N-C) + ν (C-C) + ν (O-C) dipeptide	
810	799	38	τ_{oop} (H-C-C-C) batho	
768	743	48	τ (O-C-N-C) dipeptide	
740	732	48	τ_{oop} (H-C-C-C) batho	
	732	29	τ (C-C-C-C) batho	
	731	44	τ_{oop} (H-C-C-C) batho	
	731	28	τ (C-C-C-C) batho	
704	682	61	δ (C-C-O) dipeptide	
666	640	39	δ (C-C-C) batho	
630	632	28	δ (C-C-C) batho	
598	581	47	τ (H-N-C-C) dipeptide	
575	564	64	τ (O-C-O-C) dipeptide	
548	543	26	δ (C-C-N) dipeptide	
521	507	52	δ (C-C-N) + δ (C-C-O) + δ (O-C-O) dipeptide	
438	428	37	τ (C-N-C-C) dipeptide	
417	421	74	τ (C-C-C-C) batho	
	420	72	τ (C-C-C-C) batho	

Despite being performed in the gas phase, calculations led to a good agreement between experimental and calculated values accounting for the validity of the computational model. The differences between the calculated and experimental frequencies regarding the N-H stretching, in which the experimental frequencies are lower, are possibly due to the participation of these bonds in intermolecular H bonding in the solid state that is unaccounted for in the gas phase model.

2.2. Solid-State Characterization: Infrared Spectra

All the studied heteroleptic complexes present similar infrared spectra. IR spectra of the obtained complexes were assigned taking into account the calculated IR and interpretation for compound **3**, as well as the previously reported data for related complexes [18,20,22–26]. The common characteristic bands in the spectra (Table 2), include a broad, very strong peak at approximately 1600 cm^{-1} corresponding to $\nu(\text{C}=\text{O}) + \nu(\text{C}-\text{N}) + \nu_{\text{as}}(\text{COO})$, which is characteristic of the coordinated dipeptide moiety. This broad peak is superimposed on the one assigned to the batho ring $\nu(\text{C}-\text{C})$ stretching. Absorption peaks corresponding to other ring stretching frequencies of the batho are modified in relation to the free ligand and very close to those of the $[\text{Cu}_2\text{Cl}_4(\text{batho})_2]\cdot\text{H}_2\text{O}$ (Cu-batho) appearing at approximately 1530 and 1400 cm^{-1} , in agreement with the coordination of batho.

The obtained IR spectra of the complexes are very similar to those of the corresponding $[\text{Cu}(\text{dipeptide})(\text{diimine})]$ complexes whose crystal structures have been determined. For instance, Figure 3 shows the superposition of the spectra of $[\text{Cu}(\text{phe-phe})(\text{diimine})]$ with diimine phen, neo, and batho complexes. This supports the hypothesis that the coordination in all these families of complexes is the same, with relatively similar structures, as proposed in Figure 1, in agreement with the optimized structure of **3**.

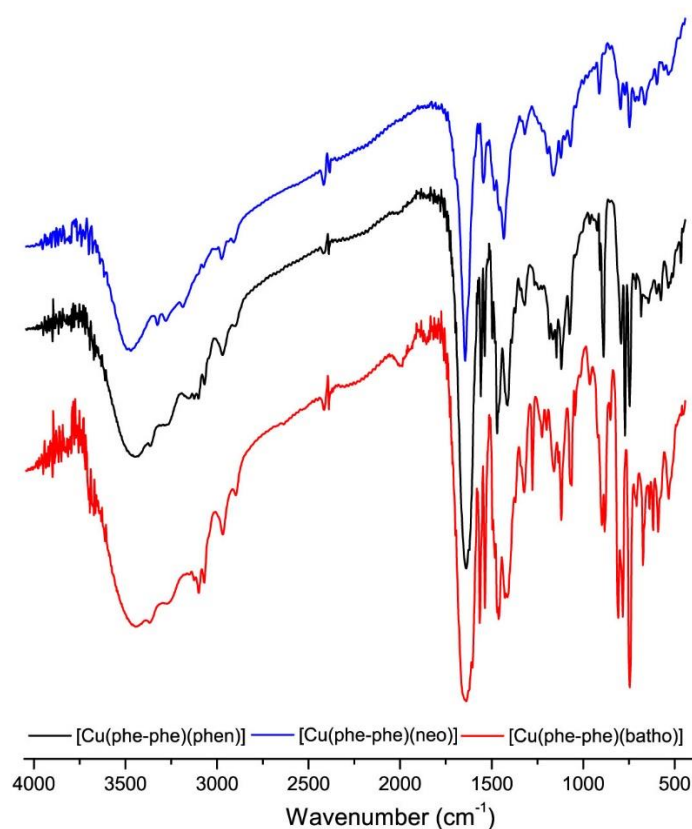


Figure 3. Superimposed IR spectra of: $[\text{Cu}(\text{L-Phe-phe})(\text{diimine})]$ with diimine: phen (black), neo (blue), and batho (red).

Table 2. FTIR spectra assignment for complexes 1–8.

Compound	$\nu_{\text{s}} + \nu_{\text{as}}(\text{N-H})^*$	$\nu(\text{C=O})^* + \nu(\text{C-N})^{**}$ $+ \nu_{\text{as}}(\text{COO})^* +$ $\nu(\text{C-C})^{**}$	$\nu(\text{N-C})^* + \nu(\text{C=O})^*$ $+ \nu(\text{C-C})^*$	$\nu_{\text{s}}(\text{COO})^* +$ $\nu(\text{C-C})^*$	$\rho(\text{C-H})^{**}$	$\delta(\text{C-C-O})^*$	$\delta(\text{C-C-N})^* +$ $\delta(\text{C-C-O})^* +$ $\delta(\text{O-C-O})^*$
1	3415sh	1588s, 1516w	1420m	1239w	1040w	704s	536w
2	3401sh	1594s, 1516w	1417m	1226w	1040w	704s	542w
3	3412sh	1597s, 1521w	1427m	1232w	1094w	704s	575w
4	3415sh	1594s, 1516w	1413m	1226w	1084w	704s	549w
5	3401sh	1601s, 1523w	1413m	1233w	1065w	704s	542w
6	3415sh	1601s, 1516w	1420m	1239w	1064w	704s	549w
7	3408sh	1594s, 1516w	1427m	1233m	1065w	704s	536w
8	3401sh	1594s, 1523w	1413m	1233m	1072w	704s	555w

* Dipeptide bands; ** batho bands.

2.3. Characterization in Solution UV–Visible Spectra

To gain insight into the major species in solution, electronic spectra of the complexes were recorded and analyzed. All complexes present a broad peak at approximately 610 nm with a shoulder at approximately 850 nm. This is typical of Cu(II) in pentacoordinate complexes. The wavelength of the maximum absorption (λ_{max}) and absorptivity values are listed in Table 3.

Table 3. Wavelength of the maximum absorption (λ_{max} , nm) and molar absorptivity (ϵ).

Compound	λ_{max} (nm) in DMSO/in Water:DMSO 50:50 *	ϵ (DMSO)
1	608	178
2	610	147
3	615/630	132
4	611	92
5	610/620	133
6	611	142
7	610	106
8	608	121

* Only for soluble compounds in this condition.

An empirical correlation between the visible spectrum λ_{max} and the donor atoms coordinated to the Cu(II) was used to analyze the experimental spectra [27,28]. The λ_{max} of the visible spectra, calculated according to *Prenci et al.* [28,29] for the coordination scheme shown in Figure 1 (corresponding to proposed solid-state coordination) is approximately 610–620 nm, similar to the experimental value in DMSO. This suggests that the pentacoordinate heteroleptic complex is the solution's major species, not excluding others' existence, as observed for [Cu(L-dipeptide)(phen)], [Cu(L-dipeptide)(neo)], and [Cu(L-dipeptide)(tmp)] complexes [18,20,22]. In a DMSO:water (50:50) solution, the same spectral characteristics were observed, with λ_{max} shifted to 620–630 nm.

There are no significant changes in spectra during 48 h (both in DMSO and DMSO:water). Therefore, complexes are stable during this period in solution. Conductivity measurements also are stable with time (values in the 0–2 μS at 1 mM in DMSO).

2.4. DNA binding

Values of intrinsic binding constants to DNA (K_b) of the homoleptic and heteroleptic complexes were similar, with values of approximately 1×10^3 (Table S1, Supplementary Materials). The K_b values are approximately ten-fold lower than those of the corresponding [Cu(L-dipeptide)(phen)] [18] and similar to those of [Cu(L-dipeptide)(tmp)] [22] complexes,

suggesting that phenyl groups impair DNA binding as compared to phen, similarly to methyl groups of tmp.

The viscosity of the DNA is highly sensitive to changes in the DNA's length. Its study is considered among the most reliable techniques for DNA binding mode analysis in solution. DNA base pairs tend to separate to accommodate an intercalated molecule into the helix, increasing the length of the DNA, leading to a viscosity increase. Other binding modes exert minor modifications on DNA viscosity [30,31].

The relative viscosity of CT-DNA in the presence of compounds 3 and 5, the homoleptic Cu-batho and free batho compounds as well as the related complexes of phen, tmp and neo were determined. Figure 4 presents the obtained results.

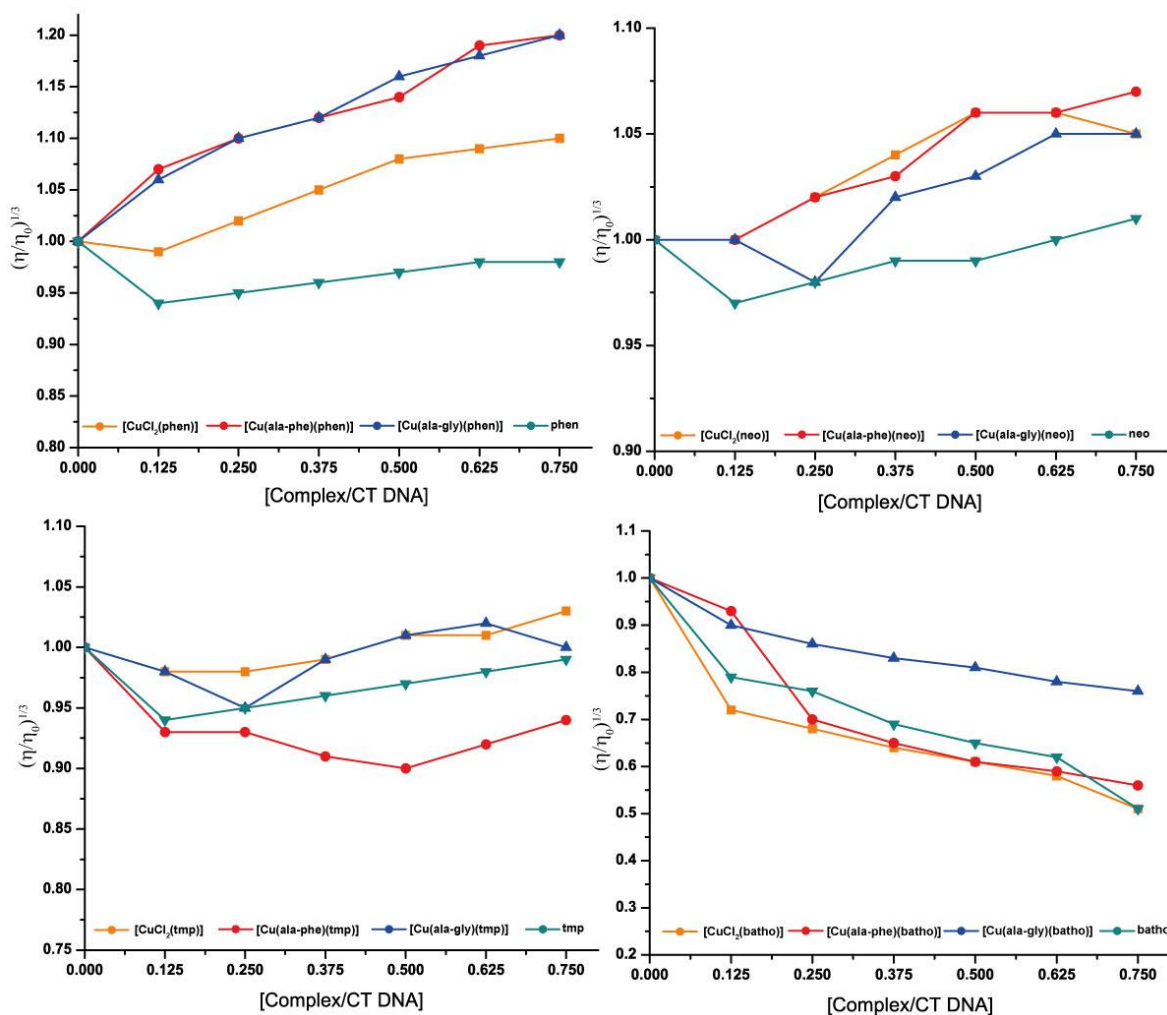


Figure 4. Effect of the increasing concentration of complexes on the relative viscosity of CT -DNA. [DNA] = 150 μ M, for the free diimine, Cu-diimine and [Cu(L-dipeptide)(diimine)] for diimine: phen, neo tmp and batho.

In relation to the free diimine DNA binding, it is observed that the relative viscosity decreases at the complex/DNA ratio of 0.125. Such behavior may be explained by a binding mode that produces bends or kinks in the DNA helix, as observed for some partial or non-classical intercalators, including the Δ -[Ru(phen)₃]²⁺ complex [32,33]. At higher complex/DNA ratios for phen, neo and tmp it slightly increases, whereas for batho it continues to decrease. This observation cannot be straightforwardly explained. It can be hypothesized that at low complex/DNA ratios, the diimine binding induces the DNA to bend. The positions for that mode of binding are saturated at ratios higher than 0.125 for phen, neo and tmp and when the diimine is present at higher ratios, it binds in a different mode.

Phen-containing complexes augmented DNA relative viscosity, with Cu-phen inducing a significant increase. The Cu-phen plot slope (0.27) is near the estimated one for a partial or non-classical intercalator [34] (the slope for ethidium bromide, a classical intercalator, is approximately 1 [31]). This agrees with the partial intercalation and groove binding to DNA detected for this complex via fiber EPR studies [35]. The heteroleptic complexes induced a similar increase in viscosity. A similar behavior was found for phen-containing complexes Casiopeinas, where both intercalation and minor groove binding are present, to different extents depending on the anionic ligand [36]. Experiments were repeated in water without using DMSO, yielding the same results. Neo and neo-containing complexes present a less marked increase in viscosity than phen complexes, possibly accounting only for groove binding (slope approximately 0.1), as detected for Cu-tmp complex by fiber EPR studies [35]. Tmp complexes induce no significant alteration of DNA viscosity. This pattern of methyl groups impairing DNA intercalation agrees with that reported by Palaniandavar et al. [37] for related $[\text{Cu}(\text{diimine})_2]^{2+}$ complexes.

Free batho and batho-containing complexes displayed a markedly different behavior. Viscosity decreased in the presence of the compounds, with a negative slope of approximately 0.3 (approximate slopes are included in Table S2, Supplementary Materials). This may result from groove binding inducing bends on the DNA (since the phenomenon is also observed for free batho covalent binding is discarded) possibly by partial intercalation of the phenyl groups of batho [31].

To sum up, phen complexes studied in this work, both homoleptic and heteroleptic, may intercalate to DNA as well as binding in the grooves. Neo and possibly tmp complexes, homoleptic and heteroleptic, do not evidence intercalation, possibly binding in the grooves. For the batho complexes (and free batho), a different pattern of viscosity changes was observed that suggests that batho binding induces bends in the DNA possibly as a result of partial intercalation of the phenyl groups.

2.5. Cytotoxicity

The complexes were highly cytotoxic against the studied cell lines, as presented in Table 4. Most complexes showed much higher activity than cisplatin on the studied cancer cells.

Table 4. Cytotoxic activity (expressed by IC_{50} in μM) of the studied complexes after 48 h of incubation, against MCF-7, MDA-MB-231 (human breast adenocarcinomas, the latter triple negative), MCF-10A (breast non-tumor), A549 (human lung epithelial carcinoma), and MRC-5 (lung non-tumor).

Compound	MDA-MB-231	MCF-7	MCF-10A	A549	MRC-5
1 [Cu(gly-val)(batho)]	0.41 ± 0.03	0.40 ± 0.01	4.95 ± 0.94	1.20 ± 0.36	0.60 ± 0.12
2 [Cu(gly-phe)(batho)]	1.16 ± 0.22	1.40 ± 0.20	5.28 ± 0.52	1.77 ± 0.22	1.72 ± 0.09
3 [Cu(ala-gly)(batho)]	5.30 ± 0.81	1.34 ± 0.80	6.67 ± 1.89	2.18 ± 0.44	0.15 ± 0.03
4 [Cu(ala-ala)(batho)]	0.47 ± 0.07	1.45 ± 0.43	3.60 ± 0.31	0.90 ± 0.07	0.61 ± 0.17
5 [Cu(ala-phe)(batho)]	0.97 ± 0.20	1.49 ± 0.46	3.86 ± 0.98	0.66 ± 0.20	0.31 ± 0.05
6 [Cu(phe-ala)(batho)]	0.79 ± 0.13	0.53 ± 0.09	1.78 ± 0.41	0.33 ± 0.13	0.25 ± 0.02
7 [Cu(phe-val)(batho)]	0.65 ± 0.06	1.54 ± 0.96	3.75 ± 0.78	1.47 ± 0.16	0.35 ± 0.05
8 [Cu(phe-phe)(batho)]	1.06 ± 0.44	3.34 ± 2.38	4.28 ± 0.75	1.59 ± 0.18	0.99 ± 0.21
0 [CuCl ₂ (batho)]	0.47 ± 0.07	2.75 ± 0.84	2.75 ± 0.60	0.87 ± 0.11	0.85 ± 0.15
Cisplatin	12.43 ± 0.20	8.91 ± 2.60	23.90 ± 0.70	14.40 ± 1.40	29.09 ± 0.78

Compared with other Cu compounds, the complexes can be classified as potent or remarkable cytotoxic agents according to the classification of Santini et al. [3] as they present IC_{50} in the low μM range. In general, complexes are highly active if compared with other heteroleptic complexes containing a phen based ligand [15], including Casiopeinas [7]. As compared with others [Cu(dipeptide)(diimines)] compounds, the cytotoxicity depends more on the diimine than on the dipeptide, with the activity increasing in the order phen \cong 5-NO₂-phen < batho <= neo <= tmp. Despite not being the more active compounds, batho complexes

are in general slightly more selective than the other [Cu(L-dipeptide)(diimine)] complexes (Table S3, Supplementary Materials). Therefore, [Cu(dipeptide)(batho)] complexes are interesting compounds to further study their biological activity especially, their anti-breast CSC activity, for instance [Cu(gly-val)(batho)] and [CuCl₂(batho)] could be tested on triple negative breast cancer.

3. Materials and Methods

All reagents for the synthesis and biochemical studies were used as purchased without further purification: copper salts (Fluka), L-dipeptides (SIGMA, Sigma-Aldrich, St. Louis, MO, USA), bathophenanthroline (4,7-diphenyl-1,10-phenanthroline, SIGMA) and calf thymus-DNA (CT-DNA, SIGMA).

3.1. Synthesis and Analytical Characterization

Firstly, the [Cu(dipeptide)] precursor was obtained by dissolving the dipeptide in the minimum volume of water. To this solution, a 50% excess of CuCO₃ (in relation to the dipeptide) was added and stirred at 60–80 °C for 1 h. After that, the remaining excess of CuCO₃ was filtered off. The resulting blue solution was evaporated at 60–80 °C until an adequate amount of solid is obtained which was then filtered, washed with cold water and air dried [24,25,38]. The L-dipeptides were: Gly-Val, Gly-Phe, Ala-Gly, Ala-Ala, Ala-Phe, Val-Phe, Phe-Ala and Phe-Phe. Equimolar amounts of [Cu(dipeptide)] in a water solution and batho in an ethanolic solution were mixed while constant stirring for 15 min at 60 °C. Amorphous solid was obtained after solvent evaporation at room temperature, with yields ranging from 50 to 70%. Several attempts were unsuccessful in obtaining single crystals by varying the temperature and solvent mixtures.

Elemental analysis for C, N, H and S was performed in a Thermo Flash 2000 equipment and results are as follows: [Cu(L-Gly-Val)(batho)]·CH₃CH₂OH·3H₂O, **1**, Calc./Found (CuC₃₃N₄H₄₀O₇) %C: 59.31/59.62, %N: 8.38/8.26, %H: 6.03/5.62; [Cu(L-Gly-Phe)(batho)]·CH₃CH₂OH·5.5H₂O, **2**, Calc./Found (CuC₃₇N₄H₄₅O_{9.5}) %C: 58.37/58.16, %N: 7.36/7.39, %H: 5.95/5.53; [Cu(L-Ala-Gly)(batho)]·3H₂O, **3**, Calc./Found (CuC₃₁N₄H₃₄O₆) %C: 59.44/60.19, %N: 9.01/9.05, %H: 4.98/5.08; [Cu(L-Ala-Ala)(batho)]·CH₃CH₂OH·4H₂O, **4**, Calc./Found (CuC₃₂N₄H₄₀O₈) %C: 57.17/56.98, %N: 8.33/8.44, %H: 6.00/5.78; [Cu(L-Ala-Phe)(batho)]·CH₃CH₂OH·4.5H₂O, **5**, Calc./Found (CuC₃₈N₄H₄₅O_{8.5}) %C: 60.27/60.54, %N: 7.40/7.37, %H: 5.99/5.67; [Cu(L-Phe-Ala)(batho)]·1.5CH₃CH₂OH·3H₂O, **6**, Calc./Found (CuC₃₉N₄H₄₅O_{7.5}) %C: 62.18/62.30, %N: 7.44/7.55, %H: 6.02/5.69; [Cu(L-Phe-Val)(batho)]·0.5CH₃CH₂OH·10H₂O, **7**, Calc./Found (CuC₄₀N₄H₆₀O₁₄) %C: 54.44/54.51, %N: 6.68/6.60, %H: 6.59/6.22; [Cu(L-Phe-Phe)(batho)]·3CH₃CH₂OH·9H₂O, and **C8** and Calc./Found (CuC₄₇N₄H₆₆O₁₄) %C: 57.27/57.95, %N: 5.56/5.78, %H: 7.00/6.59.

3.2. DFT Studies (Geometry Optimization and Infrared Spectra)

The proposed starting geometry for the pentacoordinate compound **3** was based on the crystal structure of the previously reported phen analogue [18] and modified in Gaussview 5.0 [39]. Geometry optimization in the gas phase was performed using the density functional theory method (DFT) [40] with the B3LYP functional [41] and the LANL2DZ basis set [42–44]. Calculations were performed on Gaussian 09 software [45]. Upon completion, all determined frequencies presented real values confirming it referred to an energy minimum.

Potential energy distribution (PED) analysis was performed on the calculated infrared spectra using VEDA software [46].

3.3. Spectroscopic Characterization

Infrared spectra of the compounds in KBr pellets were recorded on a Shimadzu IR Prestige 21 spectrometer in the 4000 to 400 cm⁻¹ range using 20 accumulations and a resolution of 4 cm⁻¹.

Solution electronic (UV–vis) spectra of the complexes were carried out in a Thermo Scientific Evolution 60 spectrophotometer, using 1 cm path length quartz cells, in 5 mM DMSO solutions and in 2.5 DMSO: H₂O 50:50 (complexes are not soluble in pure H₂O).

3.4. DNA Interaction

3.4.1. Determination of K_b via the UV Absorption Titration Experiments

Absorption titration measurements were carried out keeping the complex concentration constant at 10–15 μ M in 5 mM buffer Tris/HCl pH = 7.5 and 50 mM of NaCl while varying the concentration of calf thymus-DNA (CT-DNA) from 0 to 250 μ M. The intrinsic binding constants (K_b) were determined using the Benesi–Hildebrand method [47], by calculating the ratio of the slope to the intercept of the $[\text{complex}]/A_{\text{obs}}$ as a function of $1/[\text{DNA}]$ plot.

3.4.2. Viscosity Studies

Measurements of viscosity were performed in an Ostwald-type viscosimeter maintained at a constant temperature of 25.0 ± 0.1 °C in a thermostatic bath.

Solutions of calf thymus-DNA (CT-DNA, 150 μ M b.p.) and compounds were prepared, separately in Tris-HCl (10 mM, pH = 7.2) and thermostated at 25 °C. Complex–DNA solutions were prepared just prior to running each experiment, (6 mL) at different molar ratios ($[\text{complex}]/[\text{CT-DNA}] = 0.125, 0.250, 0.375, 0.500, 0.625$ and 0.750). Solutions were equilibrated for 15 min at 25 °C and then 5 flow times were registered.

The relative viscosity of DNA in the absence (η_0) and presence (η) of complexes was calculated as: $(\eta/\eta_0) = t - t_0/t_{\text{DNA}} - t_0$, where t_0 and t_{DNA} are the flow times of the buffer and DNA solution alone, respectively, while t is the flow time of the DNA solution in the presence of copper compounds. Data are presented as $(\eta/\eta_0)^{1/3}$ versus the ratio $[\text{complex}]/[\text{DNA}]$ [48].

3.5. Cytotoxicity Studies

The cytotoxicity of the complexes was evaluated against different human cancer cell lines: human metastatic breast adenocarcinoma MDA-MB-231 (triple negative, ATCC: HTB-26), MCF-7 (hormone-dependent ATCC: HTB-22), human lung epithelial carcinoma A549 (ATCC: CCL-185) and non-tumor cell lines MRC-5 (lung; ATCC: CCL-171) and MCF-10A (breast, ATCC: CRL-10317), using the 3-(4,5-dimethylthiazol-2-yl)-2,5-diphenyltetrazolium bromide (MTT) colorimetric assay. The cells were cultured in Dulbecco's Modified Eagle's Medium (DMEM) for MDA-MB-231, A549 and MRC-5, supplemented with 10% fetal bovine serum (FBS), Roswell Park Memorial Institute (RPMI) 1640 Medium for MCF-7, supplemented with 10% FBS or Dulbecco's Modified Eagle Medium Nutrient Mixture F-12 (DMEM F-12) for MCF-10A, containing 5% horse serum, Epidermal growth factor (EGF, 20 ng mL⁻¹), hydrocortisone (0.5 μ g mL⁻¹), insulin (0.01 mg mL⁻¹), 1% penicillin and 1% streptomycin, at 310 K in humidified 5% CO₂ atmosphere. To conduct the assay, 1.5×10^4 cells/well were seeded in 150 μ L of medium in 96-well plates and incubated at 310 K in 5% CO₂ for 24 h to allow cell adhesion. Then, the cells were treated with copper complexes for 48 h. Cu complexes were dissolved in DMSO, and 0.75 μ L of solution was added to each well with 150 μ L of medium (final concentration of 0.5% DMSO/well). Cisplatin, used as a reference drug, was solubilized in DMF. After the treatment, MTT (50 μ L, 1 mg mL⁻¹ in PBS) was added to each well, and the plate was incubated for 3 h. Cell viability was detected by the reduction of MTT to purple formazan by living cells. The formazan crystals were solubilized by isopropanol (150 μ L/well), and the optical density of each well was measured using a microplate spectrophotometer at a wavelength of 540 nm. The concentration to 50% (IC₅₀) of cell viability (Table 4) was obtained from the analysis of absorbance data of three independent experiments.

4. Conclusions

Eight new heteroleptic [Cu(L-dipeptide)(batho)] complexes were synthesized and characterized both in the solid state and in solution. The coordination environment of the metal in the solid state is maintained in the major species in solution and is the same as in other [Cu(L-dipeptide)(diimine)] compounds.

The complexes are highly cytotoxic as compared with other Cu complexes and cisplatin, and are interesting candidates to further study their anti-CSC activity and their *in vivo* activity.

Batho impairs DNA binding as compared to phen complexes, possibly favoring (major) groove binding, with the dipeptide only modulating the strength of the binding. In spite of that, the introduction of batho as a ligand augmented the cytotoxic activity of the complexes, as compared to the [Cu(L-dipeptide)(phen)], suggesting that the DNA intercalation is not determinant in the cytotoxicity of the compounds.

Supplementary Materials: The following supporting information can be downloaded at: <https://www.mdpi.com/article/10.3390/molecules28020896/s1>, Figure S1: Space fill representation of the optimized structure of compound 3. Table S1: DNA binding constants (K_b) determined by the Benesi–Hildebrand method. For comparison, previously determined values of related complexes are also included. Table S2: Approximate DNA slope of the variation of the viscosity induced by the binding of the complexes. Table S3: Selectivity index of the compounds (SI, IC_{50} on non-tumor cells/ IC_{50} on tumor cells of related origin).

Author Contributions: Conceptualization, G.F.; methodology, G.F. and A.A.B.; validation, G.F.; formal analysis, N.A.; investigation, C.Y.F., A.R. and N.A.; resources, G.F.; data curation, N.A. and C.Y.F.; writing—original draft preparation, G.F.; writing—review and editing, G.F., N.A., J.E., A.A.B. and A.J.C.-F.; visualization, N.A. and C.Y.F.; supervision, G.F.; project administration, G.F.; funding acquisition, G.F., J.E. and A.A.B. All authors have read and agreed to the published version of the manuscript.

Funding: This research was funded by Comisión Sectorial de Investigación Científica (CSIC Uruguay, I+D 2018 grant to G.F.) and also Programa de Desarrollo de las Ciencias Básicas (PEDECIBA Química), Uruguay and Fundação de Amparo à Pesquisa do Estado de São Paulo (FAPESP) and Conselho Nacional de Desenvolvimento Científico e Tecnológico (CNPq), Brazil.

Data Availability Statement: The data presented in this study are available in the article and supplementary material.

Conflicts of Interest: The authors declare that they have no conflict of interest.

References

1. Sung, H.; Ferlay, J.; Siegel, R.L.; Laversanne, M.; Soerjomataram, I.; Jemal, A.; Bray, F. Global Cancer Statistics 2020: GLOBOCAN Estimates of Incidence and Mortality Worldwide for 36 Cancers in 185 Countries. *CA Cancer J. Clin.* **2021**, *71*, 209–249. [CrossRef]
2. Chandrashekar, M.; Nayak, V.L.; Ramakrishna, S.; Mallavadhani, U.V. Novel triazole hybrids of myrrhanone C, a natural polygodane triterpene: Synthesis, cytotoxic activity and cell based studies. *Eur. J. Med. Chem.* **2016**, *114*, 293–307. [CrossRef]
3. Santini, C.; Pellei, M.; Gandin, V.; Porchia, M.; Tisato, F.; Marzano, C. Advances in Copper Complexes as Anticancer Agents. *Chem. Rev.* **2014**, *114*, 815–862. [CrossRef] [PubMed]
4. Kellett, A.; Molphy, Z.; McKee, V.; Slator, C. Recent Advances in Anticancer Copper Compounds. In *Metal-Based Anticancer Agents*; RSC Publishing: Cambridge, UK, 2019; pp. 91–119.
5. Van Rijt, S.H.; Sadler, P.J. Current applications and future potential for bioinorganic chemistry in the development of anticancer drugs. *Drug Discov. Today* **2009**, *14*, 1089–1097. [CrossRef] [PubMed]
6. Casini, A.; Vessières, A.; Meier-Menches, S.M. *Metal-Based Anticancer Agents*; Royal Society of Chemistry: London, UK, 2019; Volume 14.
7. Figueroa-DePaz, Y.; Pérez-Villanueva, J.; Soria-Arteche, O.; Martínez-Otero, D.; Gómez-Vidales, V.; Ortiz-Frade, L.; Ruiz-Azuara, L. Casiopeinas of Third Generations: Synthesis, Characterization, Cytotoxic Activity and Structure—Activity Relationships of Mixed Chelate Compounds with Bioactive Secondary Ligands. *Molecules* **2022**, *27*, 3504. [PubMed]
8. Aguilar-Jimenez, Z.; Gonzalez-Ballesteros, M.; Davila-Manzanilla, S.G.; Espinoza-Guillen, A.; Ruiz-Azuara, L. Development and In Vitro and In Vivo Evaluation of an Antineoplastic Copper(II) Compound (Casiopeina III-ia) Loaded in Nonionic Vesicles Using Quality by Design. *Int. J. Mol. Sci.* **2022**, *23*, 12756. [CrossRef] [PubMed]
9. Marzano, C.; Gandin, V.; Pellei, M.; Colavito, D.; Papini, G.; Lobbia, G.G.; Del Giudice, E.; Porchia, M.; Tisato, F.; Santini, C. In vitro antitumor activity of the water soluble copper(I) complexes bearing the tris(hydroxymethyl)phosphine ligand. *J. Med. Chem.* **2008**, *51*, 798–808. [CrossRef]

10. Gandin, V.; Ceresa, C.; Esposito, G.; Indraccolo, S.; Porchia, M.; Tisato, F.; Santini, C.; Pellei, M.; Marzano, C. Therapeutic potential of the phosphino Cu(I) complex (HydroCuP) in the treatment of solid tumors. *Sci. Rep.* **2017**, *7*, 13936. [[CrossRef](#)] [[PubMed](#)]
11. Ceresa, C.; Nicolini, G.; Semperboni, S.; Gandin, V.; Monfrini, M.; Avezza, F.; Alberti, P.; Bravin, A.; Pellei, M.; Santini, C.; et al. Evaluation of the Profile and Mechanism of Neurotoxicity of Water-Soluble [Cu(P)(4)]PF(6) and [Au(P)(4)]PF(6) (P = thp or PTA) Anticancer Complexes. *Neurotox. Res.* **2018**, *34*, 93–108. [[CrossRef](#)]
12. Northcote-Smith, J.; Kaur, P.; Suntharalingam, K. A Cancer Stem Cell Potent Copper(II) Complex with a S, N, S-Schiff base Ligand and Bathophenanthroline. *Eur. J. Inorg. Chem.* **2021**, *2021*, 1770–1775. [[CrossRef](#)]
13. Kaur, P.; Johnson, A.; Northcote-Smith, J.; Lu, C.; Suntharalingam, K. Immunogenic Cell Death of Breast Cancer Stem Cells Induced by an Endoplasmic Reticulum-Targeting Copper(II) Complex. *ChemBioChem* **2020**, *21*, 3618–3624. [[CrossRef](#)]
14. Mejía, C.; Ortega-Rosales, S.; Ruiz-Azuara, L. Mechanism of Action of Anticancer Metallodrugs. In *Biomedical Applications of Metals*; Springer: Cham, Switzerland, 2018; pp. 213–234.
15. Masuri, S.; Vañhara, P.; Cabiddu, M.G.; Morán, L.; Havel, J.; Cadoni, E.; Pivetta, T. Copper(II) Phenanthroline-Based Complexes as Potential AntiCancer Drugs: A Walkthrough on the Mechanisms of Action. *Molecules* **2022**, *27*, 49. [[CrossRef](#)]
16. Molinaro, C.; Martoriati, A.; Pelinski, L.; Cailliau, K. Copper Complexes as Anticancer Agents Targeting Topoisomerases I and II. *Cancers* **2020**, *12*, 2863. [[CrossRef](#)] [[PubMed](#)]
17. Tsvetkov, P.; Coy, S.; Petrova, B.; Dreishpoon, M.; Verma, A.; Abdusamad, M.; Rossen, J.; Joesch-Cohen, L.; Humeidi, R.; Spangler, R.D.; et al. Copper induces cell death by targeting lipoylated TCA cycle proteins. *Science* **2022**, *375*, 1254–1261. [[CrossRef](#)]
18. Iglesias, S.; Alvarez, N.; Torre, M.H.; Kremer, E.; Ellena, J.; Ribeiro, R.R.; Barroso, R.P.; Costa-Filho, A.J.; Kramer, M.G.; Facchin, G. Synthesis, structural characterization and cytotoxic activity of ternary copper (II)-dipeptide-phenanthroline complexes. A step towards the development of new copper compounds for the treatment of cancer. *J. Inorg. Biochem.* **2014**, *139*, 117–123. [[CrossRef](#)]
19. Iglesias, S.; Alvarez, N.; Kramer, G.; Torre, M.H.; Kremer, E.; Ellena, J.; Costa-Filho, A.J.; Facchin, G. Structural Characterization and Cytotoxic Activity of Heteroleptic Copper (II) Complexes with L-Dipeptides and 5-NO₂-Phenanthroline. Crystal Structure of [Cu (Phe-Ala)(5-NO₂-Phen)]. 4H₂O. *Struct. Chem. Crystallogr. Commun.* **2015**, *1*, 7.
20. Alvarez, N.; Viña, D.; Leite, C.M.; Mendes, L.F.; Batista, A.A.; Ellena, J.; Costa-Filho, A.J.; Facchin, G. Synthesis and structural characterization of a series of ternary copper (II)-L-dipeptide-neocuproine complexes. Study of their cytotoxicity against cancer cells including MDA-MB-231, triple negative breast cancer cells. *J. Inorg. Biochem.* **2020**, *203*, 110930. [[CrossRef](#)] [[PubMed](#)]
21. Veiga, N.; Alvarez, N.; Castellano, E.E.; Ellena, J.; Facchin, G.; Torre, M.H. Comparative Study of Antioxidant and Pro-Oxidant Properties of Homoleptic and Heteroleptic Copper Complexes with Amino Acids, Dipeptides and 1,10-Phenanthroline: The Quest for Antitumor Compounds. *Molecules* **2021**, *26*, 6520. [[CrossRef](#)] [[PubMed](#)]
22. Alvarez, N.; Leite, C.M.; Napoleone, A.; Mendes, L.F.S.; Fernandez, C.Y.; Ribeiro, R.R.; Ellena, J.; Batista, A.A.; Costa-Filho, A.J.; Facchin, G. Tetramethyl-phenanthroline copper complexes in the development of drugs to treat cancer: Synthesis, characterization and cytotoxicity studies of a series of copper(II)-L-dipeptide-3,4,7,8-tetramethyl-phenanthroline complexes. *J. Biol. Inorg. Chem.* **2022**, *27*, 431–441. [[CrossRef](#)]
23. Facchin, G.; Veiga, N.; Kramer, M.G.; Batista, A.A.; Várnagy, K.; Farkas, E.; Moreno, V.; Torre, M.H. Experimental and theoretical studies of copper complexes with isomeric dipeptides as novel candidates against breast cancer. *J. Inorg. Biochem.* **2016**, *162*, 52–61. [[CrossRef](#)]
24. Facchin, G.; Torre, M.H.; Kremer, E.; Piro, O.E.; Castellano, E.E.; Baran, E.J. Structural and spectroscopic characterization of two new Cu (II)-dipeptide complexes. *Z. Fur Nat. B* **2000**, *55*, 1157–1162. [[CrossRef](#)]
25. Facchin, G.; Torre, M.H.; Kremer, E.; Piro, O.E.; Castellano, E.E.; Baran, E.J. Synthesis and characterization of three new Cu(II)-dipeptide complexes. *J. Inorg. Biochem.* **2002**, *89*, 174–180. [[CrossRef](#)] [[PubMed](#)]
26. Facchin, G.; Torre, M.; Kremer, E.; Baran, E.; Mombrú, A.; Pardo, H.; Araujo, M.; Batista, A.; Costa-Filho, A. Cu (II) complexation with His–Gly and His–Ala. X-ray structure of [Cu (his–gly)₂(H₂O)₂] · 6H₂O. *Inorg. Chim. Acta* **2003**, *355*, 408–413. [[CrossRef](#)]
27. Sigel, H.; Martin, R.B. Coordinating properties of the amide bond. Stability and structure of metal ion complexes of peptides and related ligands. *Chem. Rev.* **1982**, *82*, 385–426. [[CrossRef](#)]
28. Prenesti, E.; Daniele, P.; Prencipe, M.; Ostacoli, G. Spectrum–structure correlation for visible absorption spectra of copper (II) complexes in aqueous solution. *Polyhedron* **1999**, *18*, 3233–3241. [[CrossRef](#)]
29. Prenesti, E.; Daniele, P.G.; Berto, S.; Toso, S. Spectrum–structure correlation for visible absorption spectra of copper (II) complexes showing axial co-ordination in aqueous solution. *Polyhedron* **2006**, *25*, 2815–2823. [[CrossRef](#)]
30. Rehman, S.U.; Sarwar, T.; Husain, M.A.; Ishqi, H.M.; Tabish, M. Studying non-covalent drug-DNA interactions. *Arch. Biochem. Biophys.* **2015**, *576*, 49–60. [[CrossRef](#)] [[PubMed](#)]
31. Suh, D.; Chaires, J.B. Criteria for the mode of binding of DNA binding agents. *Bioorg. Med. Chem.* **1995**, *3*, 723–728. [[CrossRef](#)]
32. Satyanarayana, S.; Dabrowiak, J.C.; Chaires, J.B. Neither delta- nor lambda-tris(phenanthroline)ruthenium(II) binds to DNA by classical intercalation. *Biochemistry* **1992**, *31*, 9319–9324. [[CrossRef](#)] [[PubMed](#)]
33. Kapicak, L.; Gabbay, E.J. Effect of aromatic cations on the tertiary structure of deoxyribonucleic acid. *J. Am. Chem. Soc.* **1975**, *97*, 403–408. [[CrossRef](#)]
34. Gratal, P.; Arias-Perez, M.S.; Gude, L. 1H-imidazo[4,5-f][1,10]phenanthroline carbohydrate conjugates: Synthesis, DNA interactions and cytotoxic activity. *Bioorg. Chem.* **2022**, *125*, 105851. [[CrossRef](#)]
35. Chikira, M.; Ng, C.H.; Palaniandavar, M. Interaction of DNA with Simple and Mixed Ligand Copper (II) Complexes of 1, 10-Phenanthrolines as Studied by DNA-Fiber EPR Spectroscopy. *Int. J. Mol. Sci.* **2015**, *16*, 22754–22780. [[CrossRef](#)] [[PubMed](#)]

36. Figueroa-DePaz, Y.; Resendiz-Acevedo, K.; Davila-Manzanilla, S.G.; Garcia-Ramos, J.C.; Ortiz-Frade, L.; Serment-Guerrero, J.; Ruiz-Azuara, L. DNA, a target of mixed chelate copper(II) compounds (Casiopeinas(R)) studied by electrophoresis, UV-vis and circular dichroism techniques. *J. Inorg. Biochem.* **2022**, *231*, 111772. [[CrossRef](#)]
37. Mahadevan, S.; Palaniandavar, M. Spectral and Electrochemical Behavior of Copper(II)-Phenanthrolines Bound to Calf Thymus DNA. [(5,6-dimethyl-OP)(2)Cu](2+) (5,6-dimethyl-OP = 5,6-Dimethyl-1,10-phenanthroline) Induces a Conformational Transition from B to Z DNA. *Inorg. Chem.* **1998**, *37*, 3927–3934. [[CrossRef](#)]
38. Facchin, G.; Kremer, E.; Baran, E.J.; Castellano, E.E.; Piro, O.E.; Ellena, J.; Costa-Filho, A.J.; Torre, M.H. Structural characterization of a series of new Cu-dipeptide complexes in solid state and in solution. *Polyhedron* **2006**, *25*, 2597–2604. [[CrossRef](#)]
39. Dennington, R.; Keith, T.; Millam, J. *GaussView, 5.0*; Semichem Inc.: Shawnee Mission, KS, USA, 2009.
40. Lewars, E.G. Introduction to Quantum Mechanics in Computational Chemistry. In *Computational Chemistry: Introduction to the Theory and Applications of Molecular and Quantum Mechanics*; Springer International Publishing: Cham, Switzerland, 2016; pp. 101–191.
41. Lee, C.; Yang, W.; Parr, R.G. Development of the Colle-Salvetti correlation-energy formula into a functional of the electron density. *Phys. Rev. B Condens. Matter* **1988**, *37*, 785–789. [[CrossRef](#)] [[PubMed](#)]
42. Wadt, W.R.; Hay, P.J. Ab initio effective core potentials for molecular calculations. Potentials for main group elements Na to Bi. *J. Chem. Phys.* **1985**, *82*, 284–298. [[CrossRef](#)]
43. Hay, P.J.; Wadt, W.R. Ab initio effective core potentials for molecular calculations. Potentials for K to Au including the outermost core orbitals. *J. Chem. Phys.* **1985**, *82*, 299–310. [[CrossRef](#)]
44. Hay, P.J.; Wadt, W.R. Ab initio effective core potentials for molecular calculations. Potentials for the transition metal atoms Sc to Hg. *J. Chem. Phys.* **1985**, *82*, 270–283. [[CrossRef](#)]
45. Frisch, M.J.; Trucks, G.W.; Schlegel, H.B.; Scuseria, G.E.; Robb, M.A.; Cheeseman, J.R.; Scalmani, G.; Barone, V.; Mennucci, B.; Petersson, G.A.; et al. *Gaussian 09*; Gaussian, Inc.: Wallingford, CT, USA, 2009.
46. Jamróz, M.H. Vibrational Energy Distribution Analysis (VEDA): Scopes and limitations. *Spectrochim. Acta Part A Mol. Biomol. Spectrosc.* **2013**, *114*, 220–230. [[CrossRef](#)]
47. Benesi, H.A.; Hildebrand, J.H. A Spectrophotometric Investigation of the Interaction of Iodine with Aromatic Hydrocarbons. *J. Am. Chem. Soc.* **2002**, *71*, 2703–2707. [[CrossRef](#)]
48. Scruggs, R.L.; Ross, P.D. Viscosity study of DNA. *Biopolymers* **1964**, *2*, 593–609. [[CrossRef](#)]

Disclaimer/Publisher's Note: The statements, opinions and data contained in all publications are solely those of the individual author(s) and contributor(s) and not of MDPI and/or the editor(s). MDPI and/or the editor(s) disclaim responsibility for any injury to people or property resulting from any ideas, methods, instructions or products referred to in the content.